A new fuzzy design for switching gain adaptation of sliding mode controller for a wind energy conversion system using a doubly fed induction generator

Mohamed Horch, Abdelkari Chemi, Lotfi Baghli, Sara Kadi

▶ **To cite this version:**

Mohamed Horch, Abdelkari Chemi, Lotfi Baghli, Sara Kadi. A new fuzzy design for switching gain adaptation of sliding mode controller for a wind energy conversion system using a doubly fed induction generator. Archives of Electrical Engineering, 2023, 72 (1), pp.273-291. 10.24425/aee.2023.143702 . hal-04060581

HAL Id: hal-04060581

https://hal.univ-lorraine.fr/hal-04060581

Submitted on 6 Apr 2023

HAL is a multi-disciplinary open access archive for the deposit and dissemination of scientific research documents, whether they are published or not. The documents may come from teaching and research institutions in France or abroad, or from public or private research centers.

L'archive ouverte pluridisciplinaire **HAL**, est destinée au dépôt et à la diffusion de documents scientifiques de niveau recherche, publiés ou non, émanant des établissements d'enseignement et de recherche français ou étrangers, des laboratoires publics ou privés.

Distributed under a Creative Commons Attribution - NonCommercial - NoDerivatives 4.0 International License

ARCHIVES OF ELECTRICAL ENGINEERING VOL. 72(1), pp. 273–291 (2023)

DOI 10.24425/aee.2023.143702

A new fuzzy design for switching gain adaptation of sliding mode controller for a wind energy conversion system using a doubly fed induction generator

MOHAMED HORCH[1] ✉, ABDELKARIM CHEMIDI[2], LOTFI BAGHLI[3], SARA KADI[4]

[1]*Laboratoire d'Automatique de Tlemcen (LAT)*
National School of Electrical and Energetic Engineering of Oran
Oran 31000, Algeria

[2]*Manufacturing Engineering Laboratory of Tlemcen*
Hight School of Applied Sciences
Tlemcen 13000, Algeria

[3]*Laboratoire d'Automatique de Tlemcen (LAT)*
Université de Lorraine
GREEN, EA 4366F-54500, Vandoeuvre-lès-Nancy, France

[4]*Laboratory of Power Equipment Characterization and Diagnosis*
University of Science and Technology Houari Boumediene
Algiers 16000, Algeria

e-mail: {✉mohamed.horch/abdelkarim.chemidi}@univ-tlemcen.dz, Lotfi.Baghli@univ-lorraine.fr, kadisara.usthb@gmail.com

(Received: 06.06.2022, revised: 28.11.2022)

Abstract: The paper proposes a new robust fuzzy gain adaptation of the sliding mode (SMC) power control strategy for the wind energy conversion system (WECS), based on a doubly fed induction generator (DFIG), to maximize the power extracted from the wind turbine (WT). The sliding mode controller can deal with any wind speed, ingrained nonlinearities in the system, external disturbances and model uncertainties, yet the chattering phenomenon that characterizes classical SMC can be destructive. This problem is suitably lessened by adopting adaptive fuzzy-SMC. For this proposed approach, the adaptive switching gains are adjusted by a supervisory fuzzy logic system, so the chattering impact is avoided. Moreover, the vector control of the DFIG as well as the presented one have been used to achieve the control of reactive and active power of the WECS to make the wind turbine adaptable to diverse constraints. Several numerical simulations are performed to assess the performance

© 2023. The Author(s). This is an open-access article distributed under the terms of the Creative Commons Attribution-NonCommercial-NoDerivatives License (CC BY-NC-ND 4.0, https://creativecommons.org/licenses/by-nc-nd/4.0/), which permits use, distribution, and reproduction in any medium, provided that the Article is properly cited, the use is non-commercial, and no modifications or adaptations are made.

www.czasopisma.pan.pl PAN POLSKA AKADEMIA NAUK www.journals.pan.pl

of the proposed control scheme. The results show robustness against parameter variations, excellent response characteristics with a reduced chattering phenomenon as compared with classical SMC.

Key words: chattering phenomenon, doubly fed induction generator, fuzzy logic gain adaptation, sliding mode control, vector control, wind energy conversion systems

1. Introduction

The electrical energy has become increasingly important to humanity. In fact, getting electrical energy is ensuring great living conditions and it is a basic factor for economic and industrial development. Faced with the ever-increasing demand for electricity, and distancing from the exploitation of polluting fossil fuels, many nations turned to renewable or green energies. The wind energy represents a rather large potential to replace existing power sources and to compensate the depreciation of the increasingly power demand. A WECS based on a DFIG is an interesting solution. This generator allows electricity production with variable speed, which gives better exploitation of wind resources [1].

Several control strategies appeared; among them the vector control. The principle is to make the control of the DFIG similar to DC machine control with separate excitation [2]. This control uses conventional controllers (proportional and integral actions), which do not allow in all cases to handle switching of operation modes and also parametric variations of the machine [3].

However, there are modern control techniques, especially the non-linear SMC strategy used due to its good dynamic performances, simple structure and ability to handle a wide range of operating conditions [4]. The higher switching gain value in the switching law of the SMC generates chattering, which diminishes the performances and may damage the system. With a view to obtaining high performances and robust control of the reactive and active powers generated by the DFIG, and to overcome the shortcomings of SMC, a new approach is proposed to reduce particularly the chattering effect.

This technique consists in adjusting the switching gains of SMC by fuzzy logic rules to relieve the effect of the chattering phenomenon in classical SMC. The objective is to show that the proposed strategy can improve the performance of a WECS based on a DFIG in terms of robustness against machine parameter variations, sensibility to disturbances and reference tracking.

2. Modelling of wind turbine

2.1. Mechanical power of the turbine

The power of wind kinetic energy can be determined by [5, 6]:

$$P_{\text{wind}} = 0.5\rho\pi R^2 V^3, \tag{1}$$

where: P_{wind} is the wind power, ρ is the air density, V is the wind speed and R is the blade radius.

The expression between wind speed and aerodynamic power extracted from the wind can be described as follows:

$$P_{\text{aer}} = 0.5 C_p(\lambda, \beta) \rho \pi R^2 V^3, \tag{2}$$

where P_{aer} is the aerodynamic power.

The power coefficient C_p of the wind turbine is a function of λ for both the tip-speed ratio (TSR) and β blade pitch angle given by this mathematical approximation [7]:

$$C_p(\lambda, \beta) = C_1 - C_2\,(\beta - C_3)\sin(A) - C_4\,(\lambda - C_5)\,(\beta - C_3) \tag{3}$$

with

$$C_1 = 0.5, \qquad C_2 = 0.0167, \qquad C_3 = 3, \qquad C_4 = 0.00184, \qquad C_5 = 3,$$

$$A = \frac{\pi\,(\lambda + 0.1)}{14.8 - 0.3(\beta - 2)}\,.$$

The tip-speed ratio λ is given by the following equation:

$$\lambda = \frac{\Omega_{\text{turb}} R}{V}\,, \tag{4}$$

where Ω_{turb} is the turbine rotational speed on the low-speed side of the gearbox.

Figure 1 represents the function of the power coefficient C_p with respect to the TSR λ for different pitch angles β.

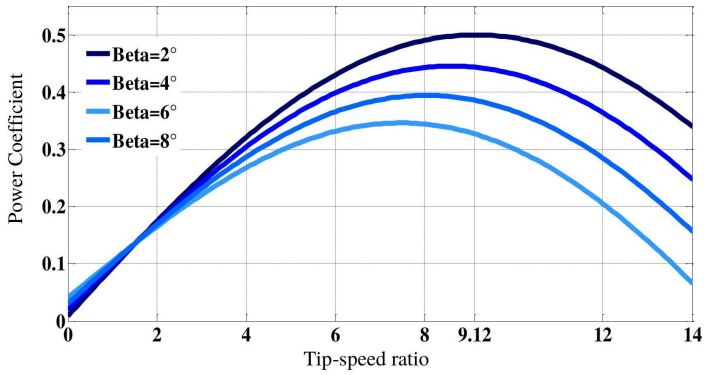

Fig. 1. Power coefficient versus tip- speed ratio for different values of the pitch angle

From this curve, we can notice that the maximum value of the power coefficient $C_p^{\max} = 0.5$ for a pitch angle $\beta = 2°$ and an optimal value of TSR $\lambda_{\text{opt}} = 9.12$. In these conditions, we can apply maximum power point tracking (MPPT) control.

The optimal turbine rotational speed from the wind $\Omega_{\text{turb}}^{\text{opt}}$ is given by:

$$\Omega_{\text{turb}}^{\text{opt}} = \frac{\lambda_{\text{opt}} R}{V}\,. \tag{5}$$

www.czasopisma.pan.pl PAN POLSKA AKADEMIA NAUK www.journals.pan.pl

The aerodynamic torque T_{aer} can be expressed as follows:

$$T_{\text{aer}} = \frac{P_{\text{aer}}}{\Omega_{\text{turb}}^{\text{opt}}} = \frac{C_p(\lambda,\beta)\rho\pi R^2 V^3}{2\Omega_{\text{turb}}^{\text{opt}}} \,. \tag{6}$$

2.2. Model of gearbox

A gearbox whose gear ratio G transforms the mechanical speed of the wind turbine Ω_{turb} into the speed of the generator shaft Ω_g and the aerodynamic torque T_{aer} into the torque generator T_g according to the following mathematical formulas:

$$\begin{cases} G = \dfrac{\Omega_g}{\Omega_{\text{turb}}} \\ G = \dfrac{T_{\text{aer}}}{T_g} \end{cases} . \tag{7}$$

2.3. Dynamic model of shaft

The fundamental equation of the dynamics makes it possible to determine the evolution of the mechanical speed from the mechanical torque exerted on the shaft of the wind turbine rotor T_g and the electromagnetic torque T_{em} [8, 9]:

$$J\frac{\mathrm{d}\Omega_g}{\mathrm{d}t} = T_g - T_{em} - f\Omega_g \,, \tag{8}$$

where: J is the total moment of inertia, f is the viscous friction coefficient, respectively.

The total inertia J consisting of the inertia of the generator J_g and the turbine inertia J_{turb}:

$$J = \frac{J_{\text{turb}}}{G^2} + J_g \,. \tag{9}$$

3. Wind speed modeling

The definition of the wind model requires climatic and geographical data of the site concerned. The deterministic effects and stochastic fluctuations are superimposed to form the following wind model [10]:

$$V(t) = A + \sum_{i=1}^{n} a_i \sin\left(\omega_i t + \varphi_i\right) , \tag{10}$$

where: φ_i is the initial phase of each turbulence, ω_i is the pulsation, A is the mean component and a_i is the magnitude.

In this paper, we are interested in the turbulent wind model, this model is clearly described in [11].

The proposed profile of the wind speed model is given in Fig. 2 with 12% of the turbulence intensity and 7.5 m·s^{-1} of a mean wind speed.

www.czasopisma.pan.pl PAN POLSKA AKADEMIA NAUK www.journals.pan.pl

Fig. 2. Variable wind speed profile

4. MPPT with rotor speed control loop

The MPPT control strategy consists in adjusting the torque appearing on the turbine shaft, so as to fix it at its reference speed. To achieve this, a rotor speed control loop is used. This control consists in determining the speed of the turbine, which makes it possible to obtain the maximum power generated [12]:

4.1. Application of conventional sliding mode control

With Eq. (8) of the turbine shaft given, we use the SMC algorithm to develop the control allowing the system to follow the desired trajectory, so the sliding surface is defined by [13]:

$$S_\Omega = \Omega_g^* - \Omega_g \,, \tag{11}$$

where Ω_g^* is the reference speed.

We consider the following Lyapunov candidate function [14]:

$$V = \frac{1}{2} S_\Omega^2 \,. \tag{12}$$

Its time derivative is given by:

$$\dot{V} = S_\Omega \cdot \dot{S}_\Omega \tag{13}$$

with

$$\dot{S}_\Omega = \dot{\Omega}_g^* - \dot{\Omega}_g \,. \tag{14}$$

By replacing (8) in the last equation, (14), we obtain:

$$\dot{S}_\Omega = \dot{\Omega}_g^* + \frac{1}{J} \left(T_{em} + f\Omega - T_g \right) . \tag{15}$$

Replacing T_{em} by the term $\left(T_{em}^{eq} + T_{em}^{n}\right)$ in the previous equation according to the sliding mode theory:

$$\dot{S}_\Omega = \dot{\Omega}_g^* + \frac{1}{J} \left(\left(T_{em}^{eq} + T_{em}^{n}\right) + f\Omega - T_g \right) . \tag{16}$$

During the sliding mode and in permanent regime, we have: $S_\Omega = 0$, $\dot{S}_\Omega = 0$ and $T_{em}^n = 0$, from which we extract the equivalent control expression [15]:

$$T_{em}^{eq} = -J\dot{\Omega}^* - f\Omega + T_g \,. \tag{17}$$

By replacing Expression (17) in (16) we obtain:

$$\dot{S}_\Omega = \frac{1}{J}\left(T_{em}^n\right). \tag{18}$$

To ensure the convergence of the Lyapunov function, we must set:

$$T_{em}^n = -K_\Omega \cdot \text{sign}\left(S_\Omega\right), \tag{19}$$

where K_Ω is a constant positive.

The control algorithm is defined by the relation:

$$T_{em} = T_{em}^{eq} + T_{em}^n \,. \tag{20}$$

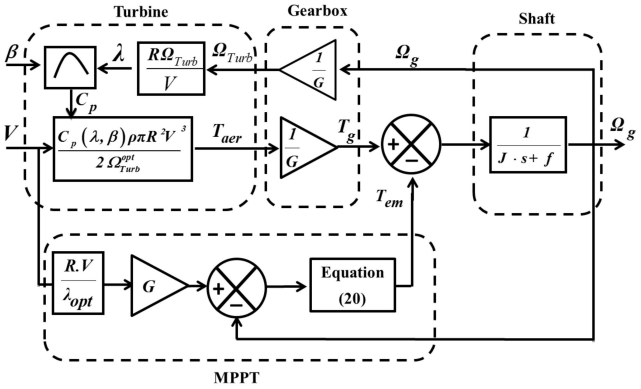

Fig. 3. Schematic-diagram of the mathematical model of turbine and MPPT with SMC control

4.2. Application of adaptive fuzzy sliding mode control

To minimize the chattering phenomenon and improve the efficiency of SMC, we propose to add the Mamdani fuzzy logic law to SMC, with the purpose of adjusting the commutation gains and attenuating its chattering [16].

When the value of the sliding surface S_Ω is important, and once the system state trajectory is distant from the sliding surface; the switching gain K_Ω must be raised to force the trajectory back. On the other hand, when the value of S_Ω is relatively small, the gain must be also minimized. However, the fuzzy-logic rules could be applied to adapt the K_Ω switching gain based on the S_Ω sliding surface values.

The fuzzy rules for both the powers and the speed controllers are presented in Table 1.

The membership-functions (MFs) of the input S_Ω and the output u_{Ω_g} signals are given in Fig. 4.

Table 1. Fuzzy logic controller rules

S_Ω	P-B	P-M	P-S	Z-E	N-S	N-M	N-B
u_{Ω_g}	P-B	P-M	P-S	Z-E	P-S	P-M	P-B

P-B: Positive-Big, P-M: Positive-Medium, P-S: Positive-Small, Z-E: Zero, N-S: Negative-Small, N-M: Negative-Medium, N-B: Negative-Big

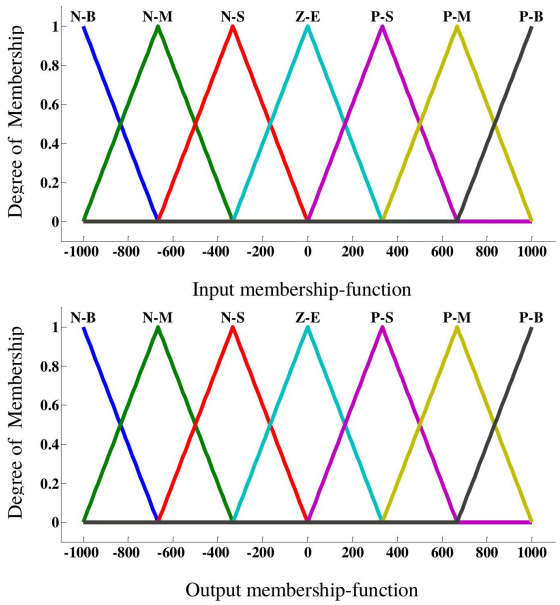

Fig. 4. The proposed membership-functions of the fuzzy logic controller inputs and outputs

Rule 1: if S_Ω is P-B, consequently u_{Ω_g} is P-B.

If S_Ω is P-B, consequently the calculated speed is significantly lower than the reference. It must be quickly increased to make it return to the reference speed, i.e., for a significant raising in the control variable u_{Ω_g} is needed. Other inference rules are similarly synthetized:

Rule 2: if S_Ω is P-M consequently u_{Ω_g} is P-M.

Rule 3: if S_Ω is P-S consequently u_{Ω_g} is P-S.

Rule 4: if S_Ω is Z-E consequently u_{Ω_g} is Z-E.

Rule 5: if S_Ω is N-S consequently u_{Ω_g} is P-S.

Rule 6: if S_Ω is N-M consequently u_{Ω_g} is P-M.

Rule 7: if S_Ω is N-B consequently u_{Ω_g} is P-B.

To obtain the switching gains of the control, the fuzzy outputs are deffuzified by using the center of the area process and multiplied by the scaling gain K_Ω. The actual gains of the controller are as follows:

$$K'_\Omega = K_\Omega \times u_{\Omega_g}. \tag{21}$$

The fuzzy-sliding-mode-controller is presented in Fig. 5.

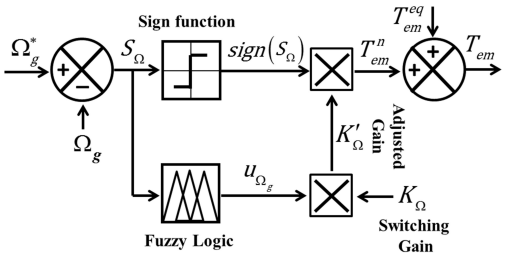

Fig. 5. Schematic-diagram of the proposed fuzzy sliding mode controller (FSMC)

4.3. Simulation results

Several simulation tests of the wind turbine system were conducted to demonstrate the feasibility of the proposed FSMC. The parameters of a wind turbine are presented in Table 6.

A random wind profile is used, corresponding to the sub-synchronous mode. The mechanical speed extracted from the MPPT controller presented in Fig. 6, varies in the same shape as the wind speed.

This MPPT technique, keeps the power-coefficient C_p at its higher value, which corresponds to 0.515 and the relative-speed stills around its optimal value $\lambda_{\text{opt}} = 9.12$.

From the mechanical speed tracking error which is almost equal to zero, the FSMC shows clearly the benefit of this algorithm in terms of chattering reduction, which is considered as one of the main disadvantages of conventional SMC.

The performance-index is a quantitative measure of the system performance. When the system achieves the lowest values, we have an optimal regulation. The performances of the wind turbine system under a random wind profile are evaluated by the various indexes for the proposed algorithms, including the IAE, ISE and ITSE in Table 2. The mathematical expressions of these indicators are [17, 18]:

Integral of absolute value of the error (IAE): This index refers to the IAE equation, (22). The total error is presented in the IAE, i.e., it shows how much the answer was with respect to the reference used.

$$\text{AE} = \int_0^\infty |e(t)|\,\mathrm{d}t. \tag{22}$$

Integral of the square error (ISE): This index is defined as the square error integral equation, (23). It is related to the energy error, offering less importance to minor errors and higher importance to larger errors.

$$\text{ISE} = \int_0^\infty [e(t)]^2\,\mathrm{d}t. \tag{23}$$

www.czasopisma.pan.pl PAN POLSKA AKADEMIA NAUK www.journals.pan.pl

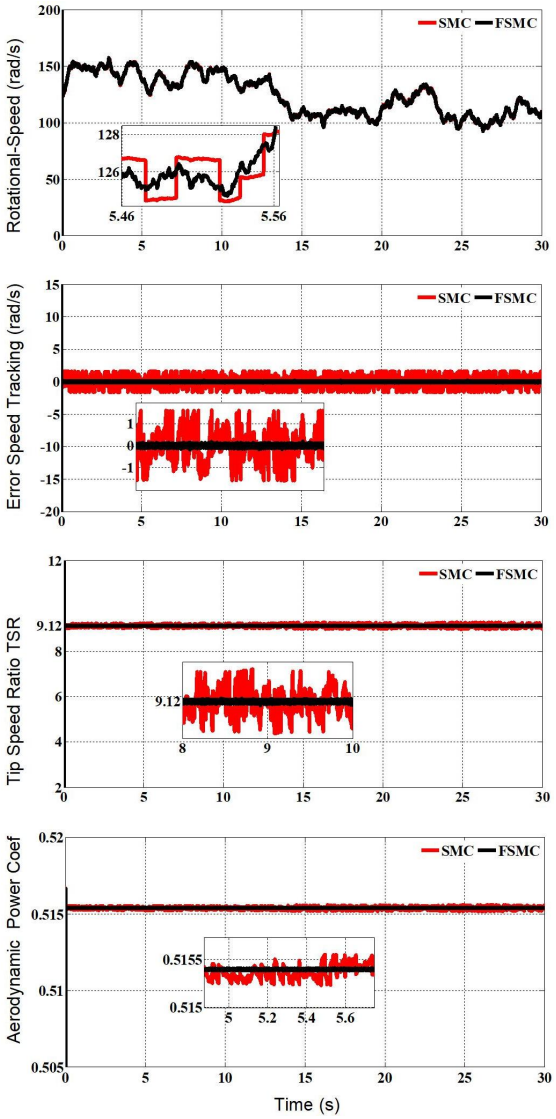

Fig. 6. Wind turbine system responses to conventional SMC and FSMC

Integral of time multiplied by the squared error (ITSE): This index is equivalent to the ISE index, but it is evaluated in time Eq. (24). The ITSE index gives very little attention to initial errors.

$$\text{ITSE} = \int_0^{\infty} t \cdot [e(t)]^2 \mathrm{d}t, \tag{24}$$

where $e(t)$ is the system response error.

As shown in Table 2, it can be stated that the FSMC algorithm achieves the smallest values of the three indices.

Table 2. Quantitative performance comparison of WT controlled by SMC and FSMC strategies

	Algorithm	**IAE**	**ISE**	**ITSE**
Ω_g	SMC	47.875	107.374	1463.797
	FSMC	**1.177**	**2.494**	**0.940**
C_p	SMC	0.018	5.696e-6	8.627e-5
	FSMC	**0.011**	**4.767e–6**	**7.062e–5**
λ	SMC	3.583	0.611	9.426
	FSMC	**0.087**	**0.013**	**0.006**

5. Modelling of DFIG

The mathematical-model of the DFIG in the $(d-q)$ frame is presented in the following equations. The stator and the rotor voltages are given by the following equations [19–21]:

$$\begin{cases} V_{sd} = R_s i_{sd} + \dfrac{\mathrm{d}(\phi_{sd})}{\mathrm{d}t} - \omega_s \phi_{sq} \\ V_{sq} = R_s i_{sq} + \dfrac{\mathrm{d}(\phi_{sq})}{\mathrm{d}t} - \omega_s \phi_{sd} \\ V_{rd} = R_r i_{rd} + \dfrac{\mathrm{d}(\phi_{rd})}{\mathrm{d}t} - \omega_r \phi_{rq} \\ V_{rq} = R_r i_{rq} + \dfrac{\mathrm{d}(\phi_{rq})}{\mathrm{d}t} - \omega_r \phi_{rd} \end{cases} \tag{25}$$

with

$$\omega_r = \omega_s p \Omega_g, \tag{26}$$

where: V_s is the stator voltage, V_r is the rotor voltage, R_s is the stator resistance, R_r is the rotor resistance, i_s is the stator current, i_r is the rotor current, ϕ_s is the stator flux, ϕ_r is the rotor flux, ω_s is the stator pulsation and ω_r is the rotor pulsation.

Equations (27) present the stator and rotor flux expressions [22]:

$$\begin{cases} \phi_{sd} = L_s i_{sd} + M i_{rd} \\ \phi_{sq} = L_s i_{sq} + M i_{rq} \\ \phi_{rd} = L_r i_{rd} + M i_{sd} \\ \phi_{rq} = L_r i_{rq} + M i_{sq} \end{cases}, \tag{27}$$

where:L_s is the stator inductance, L_r is the rotor inductance and M is the mutual inductance.

And the instant active and reactive stator powers are [23]:

$$\begin{cases} P_s = V_{sd} i_{sd} + V_{sq} i_{sq} \\ Q_s = V_{sq} i_{sd} - V_{sd} i_{sq} \end{cases}, \tag{28}$$

where P_s is the instant active power and Q_r is the instant reactive power.

The DFIG electromagnetic torque T_{eme} is defined as [24]:

$$T_{\text{eme}} = p \frac{M}{L_s} \left(\phi_{sq} i_{rd} - \phi_{sd} i_{rq} \right), \tag{29}$$

where p is the number of pole pairs.

5.1. Conventional SMC for the DFIG

After presenting the SMC theory for the MPPT control strategy in part one, the objective of this part is to control the reactive and active stator power in the DFIG, by acting on the rotor voltages. For this purpose, the control surface is determined by the following equations [25]:

$$\begin{cases} S_P = P_s^* - P_s \\ S_Q = Q_s^* - Q_s \end{cases}. \tag{30}$$

We define the derivative of the Lyapunov function by [26]:

$$\begin{cases} V\left(S_P\right) = 0.5 \left(S_P\right)^2 \\ V\left(S_Q\right) = 0.5 \left(S_Q\right)^2 \end{cases} \tag{31}$$

with

$$\begin{cases} \dot{S}_P = \dot{P}_s^* - \dot{P}_s = \dot{P}_s^* + \dfrac{L_s L_r \sigma}{V_s M} \dot{i}_{rq} \\ \dot{S}_Q = \dot{Q}_s^* - \dot{Q}_s = \dot{Q}_s^* + \dfrac{L_s L_r \sigma}{V_s M} \dot{i}_{rd} \end{cases}. \tag{32}$$

Taking the derivative of the previous equation and replacing the reactive and active power respectively:

$$\begin{cases} \dot{S}_P = +V_s \dfrac{M}{L_s L_r \sigma} \left(V_{rq} - R_r i_{rq} - \sigma L_r \omega_r i_{rd} + g \dfrac{M V_s}{\omega_s L_s} \right) \\ \dot{S}_Q = +V_s \dfrac{M}{L_s L_r \sigma} \left(V_{rd} - R_r i_{rd} + \sigma L_r \omega_r i_{rq} \right) \end{cases}, \tag{33}$$

where $g = \dfrac{\omega_s}{\omega_r}$.

Replacing i_{rq} and i_{rd} by their expressions, than V_{rq} and V_{rd} by $V_{rd}^{eq} + V_{rd}^{n}$ and $V_{rq}^{eq} + V_{rq}^{n}$, respectively, in the previous equation, the surface time derivative is given by:

$$\begin{cases} \dot{S}_P = \dot{P}_s^* + V_s \dfrac{M}{L_s L_r \sigma} \left(\left(V_{rq}^{eq} + V_{rq}^{n} \right) - R_r i_{rq} - \sigma \omega_r L_r i_{rd} + g \dfrac{M V_s}{\omega_s L_s} \right) \\ \dot{S}_Q = \dot{Q}_s^* + V_s \dfrac{M}{L_s L_r \sigma} \left(\left(V_{rd}^{eq} + V_{rd}^{n} \right) - R_r i_{rd} + \sigma \omega_r L_r i_{rq} \right) \end{cases}. \tag{34}$$

www.czasopisma.pan.pl PAN POLSKA AKADEMIA NAUK www.journals.pan.pl

During a steady state and for the sliding-mode, we have [27]:

$$\begin{cases} S_P = 0, & \dot{S}_P = 0, & V_{rq}^n = 0 \\ S_Q = 0, & \dot{S}_Q = 0, & V_{rd}^n = 0 \end{cases}. \tag{35}$$

Therefore, the equivalent control terms are given by:

$$\begin{cases} V_{rq}^{eq} = -\dfrac{\sigma L_s L_r}{V_s M}\dot{P}_s^* + R_r i_{rq} + \sigma\omega_r L_r i_{rd} - g\dfrac{MV_s}{\omega_s L_s} \\ V_{rd}^{eq} = -\dfrac{\sigma L_s L_r}{V_s M}\dot{Q}_s^* + R_r i_{rd} - \sigma\omega_r L_r i_{rq} \end{cases}. \tag{36}$$

The switching terms are written as:

$$\begin{cases} V_{rq}^n = -K_P \text{sign}\,(S_P) \\ V_{rd}^n = -K_Q \text{sign}\,(S_Q) \end{cases}. \tag{37}$$

To verify the stability-condition of the system, the two coefficients K_P and K_Q must be positive.

5.2. Adaptive fuzzy sliding mode control for the DFIG

To achieve a robust power control, the SMC controllers are replaced by adaptive FSMC as mentioned in the previous part, where the Mamdani fuzzy logic method is added to the sign function to adjust the commutation gains in order to attenuate the chattering on the active and reactive power variables.

Hence, fuzzy logic rules can be used to adjust the switching gains K_P and K_Q according to the value of S_P and S_Q, respectively. The fuzzy rules for the power controllers are shown in Table 3:

Table 3. Fuzzy logic controller rules

$S_{P,Q}$	P-B	P-M	P-S	Z-E	N-S	N-M	N-B
$u_{P,Q}$	P-B	P-M	P-S	Z-E	P-S	P-M	P-B

P-B: Positive-Big, P-M: Positive-Medium, P-S: Positive-Small, Z-E: Zero, N-S: Negative-Small, N-M: Negative-Medium, N-B: Negative-Big

The MFs of the input $S_{P,Q}$ and the output $u_{P,Q}$ signals are shown in Fig. 7.

Rule 1: if $S_{P,Q}$ is P-B, consequently $u_{P,Q}$ is P-B.

If $S_{P,Q}$ is P-B, consequently the calculated speed is significantly lower than the reference. It must be quickly increased to make it return to the reference speed, i.e., for a significant raising in the control variable $u_{P,Q}$ is needed. Other inference rules are similarly synthetized:

Rule 2: if $S_{P,Q}$ is P-M, consequently $u_{P,Q}$ is P-M.

Rule 3: if $S_{P,Q}$ is P-S, consequently $u_{P,Q}$ is P-S.

Rule 4: if $S_{P,Q}$ is Z-E, consequently $u_{P,Q}$ is Z-E.

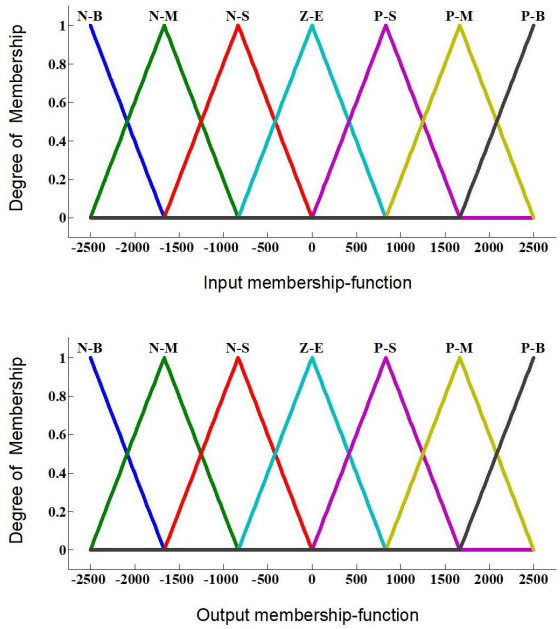

Fig. 7. The proposed membership functions of the input and output of the fuzzy logic controller

Rule 5: if $S_{P,Q}$ is N-S, consequently $u_{P,Q}$ is P-S.

Rule 6: if $S_{P,Q}$ is N-M, consequently is P-M.

Rule 7: if $S_{P,Q}$ is N-B, consequently $u_{P,Q}$ is P-B.

Additionally, to obtain the switching gains of the control, the fuzzy outputs are deffuzified by using the center of the area process and multiplied by the scaling gain K_P and K_Q. The actual gains of the controller will be:

$$\begin{cases} K'_P = K_P \times u_P \\ K'_Q = K_Q \times u_Q \end{cases}. \tag{38}$$

The control algorithm is defined by the relation:

$$\begin{cases} V^*_{rq} = V^{eq}_{rq} + V^n_{rq} \\ V^*_{rd} = V^{eq}_{rd} + V^n_{rd} \end{cases}. \tag{39}$$

The architecture of the proposed FSMC for the DFIG system is illustrated in Fig. 8.

5.3. Simulation results

The simulations are implemented using MATLAB/Simulink environment for a DFIG connected to the wind turbine mentioned in the previous section. In addition, a comparison analysis is carried out between the proposed FSMC and the conventional SMC, in terms of reference tracking (reactive and active power), and chattering phenomenon elimination.

www.czasopisma.pan.pl PAN POLSKA AKADEMIA NAUK www.journals.pan.pl

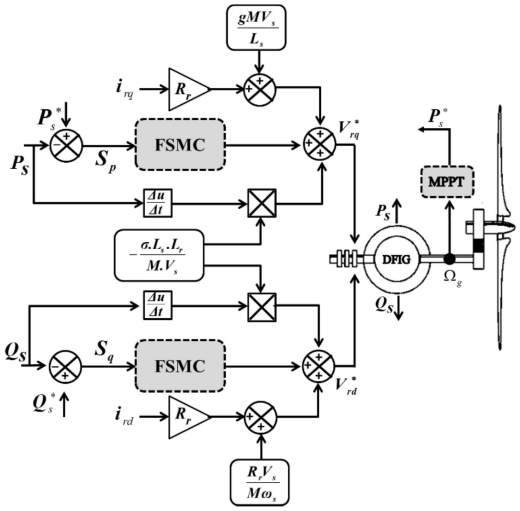

Fig. 8. Schematic-diagram of the FSMC strategy for DFIG

In this test the stator reactive power reference value will be fixed at step zero and the active power of the stator has a negative sign generated by the turbine, signifying that the generator produces energy and transmits it to the grid.

According to these results and for variable references, the stator active and reactive powers follow their changing references, whatever the wind fluctuations are, proving well maintained and perfect decoupling between the active and the reactive powers, as shown in Fig. 9.

The simulation results show high performances for both SMC and FSMC with significantly small active and reactive power errors. However, FSMC is more effective in terms of chattering attenuation.

The total-harmonic-distortion (THD) is calculated using the fast-Fourier-transform (FFT), as shown in Fig. 10. It shows the impact of the chattering phenomenon on the DFIG stator current.

The performances of the WECS under the same reference signals are evaluated by the various indices for both FSMC and conventional SMC algorithms, including the IAE, ISE, ITSE and ITAE in Table 4.

Table 4. Quantitative performance comparison of DFIG controlled by SMC and FSMC strategies

	Algorithm	**IAE**	**ISE**	**ITSE**
P_S	SMC	207.34	2 527.63	34 022.50
	FSMC	**164.59**	**1 144.86**	**22 900.90**
Q_S	SMC	201.04	8 505.79	3 091.72
	FSMC	**132.09**	**664.38**	**8 094.35**

www.czasopisma.pan.pl PAN POLSKA AKADEMIA NAUK www.journals.pan.pl

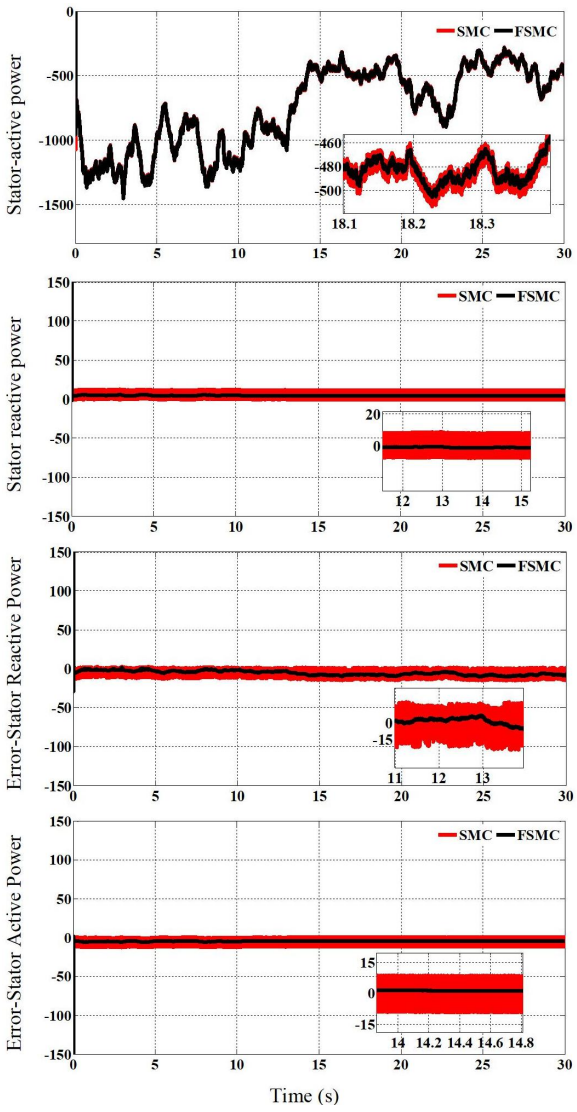

Fig. 9. WECS reference tracking test with conventional SMC and FSMC

As seen in Table 4, the FSMC algorithm offers enhanced performance by giving the smallest values of the three indexes. The THD is also reduced from 17.16% to 4.04% for the FSMC (Fig. 10). This study confirms that the FSMC has better behavior and response time, as well as optimized static and dynamic performances compared to the conventional SMC.

www.czasopisma.pan.pl PAN POLSKA AKADEMIA NAUK www.journals.pan.pl

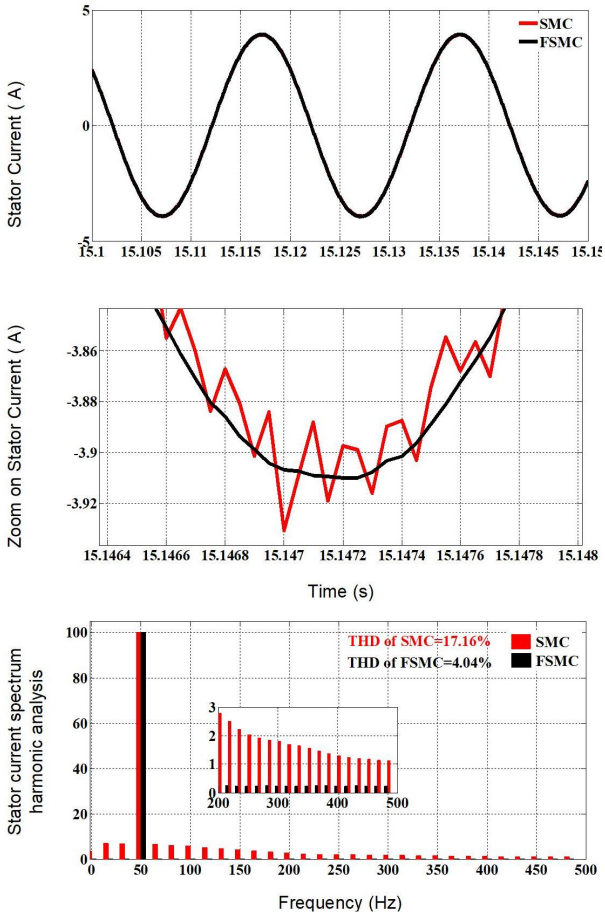

Fig. 10. Harmonic analysis of the stator-current spectrum with conventional SMC and FSMC

6. Conclusion

This paper presents a new robust fuzzy gain adaptation of the sliding mode power control strategy. The primary goal is to improve the performance of the SMC method. Different simulation scenarios for the WECS are carried under a variable-speed wind.

The results show that this fuzzy SMC is robust against parameter variations, ensures excellent response characteristics and presents almost no chattering compared to conventional SMC. The proposed strategy is also more efficient in maintaining system stability and achieving the desired performance even with various system parameters. This fuzzy sliding mode controller is a promising option for wind energy conversion systems.

www.czasopisma.pan.pl PAN POLSKA AKADEMIA NAUK www.journals.pan.pl

Appendix

Table 5. DFIG parameters

Parameters	values
P_N	7.5 kW
V_S	230/400 V
F	50 Hz
R_S	0.455 Ω
R_r	0.62 Ω
L_S	0.084 C
L_r	0.081 H
M	0.078 H
J_g	0.3125 kg·m^2
f_g	0.00673 N·m/s
p	2

Table 6. Parameters of the wind turbine

Parameters	values
P_N	10 kW
R	3 m
G	5.4
J_{turb}	0.042 kg·m^2
f	0.017 N·m/s

Acknowledgements

This work is supported by the Direction Générale de la Recherche Scientifique et du Développement Technologique (DGRSDT).

References

[1] Chemidi A., Horch M., Bourouis M.E.A., *A new robust RST controller based on PSO optimization for DFIG wind turbine*, European Journal of Electrical Engineering, vol. 24, no. 1, pp. 13–20 (2022), DOI: 10.18280/ejee.240102.

[2] Hadji C., Khodja D.E., Chakroune S., *Sensorless backstepping control using a Luenberger o server for double-star induction motor*, Archives of Electrical Engineering, vol. 69, no. 1, pp. 101–116 (2020), DOI: 10.24425/aee.2020.131761.

www.czasopisma.pan.pl PAN POLSKA AKADEMIA NAUK www.journals.pan.pl

[3] Liu S., Han Y., Du C., Li S., Zhang H., *Fuzzy PI Control for Grid-side Converter of DFIG-based Wind Turbine System*, Proceedings of 40th Chinese Control Conference (CCC), Shanghai, China, pp. 5788–5793 (2021), DOI: 10.23919/CCC52363.2021.9550601.

[4] Benbouhenni H., Bizon N., *Third-Order Sliding Mode Applied to the Direct Field-Oriented Control of the Asynchronous Generator for Variable-Speed Contra-Rotating Wind Turbine Generation Systems*, Energies, vol. 14, no. 18, p. 5877, DOI: 10.3390/en14185877.

[5] Saidi Y., Mezouar A., Miloud Y., *Advanced non-linear backstepping control design for variable speed wind turbine power maximization based on tip-speed-ratio approach during partial load operation*, International Journal of Dynamics and Control, vol. 8, pp. 615–628 (2020), DOI: 10.1007/s40435-019-00564-3.

[6] Eisa SA., Wedeward K., Stone W., *Wind turbines control system: nonlinear modeling, simulation, two and three time scale approximations, and data validation*, International Journal of Dynamics and Control, vol. 6, no. 4, pp. 1776–1798 (2018), DOI: 10.1007/s40435-018-0420-4.

[7] Javed U., Arshad M.A., Jawad M., Shabbir N., Kütt L and Rassõlkin A., *Active and Reactive Power Control of DFIG using Optimized Fractional Order-PI Controller*, IEEE 19th International Power Electronics and Motion Control Conference (PEMC), Gliwice, Poland, pp. 398–404 (2021), DOI: 10.1109/PEMC48073.2021.9432608.

[8] Dekali Z., Baghli L., Boumediene A., *Improved Super Twisting Based High Order Direct Power Sliding Mode Control of a Connected DFIG Variable Speed Wind Turbine*, Periodica Polytechnica Electrical Engineering and Computer Science, vol. 65, no. 4, pp. 352–372 (2021), DOI: 10.3311/PPee.17989.

[9] Blaabjerg F., Xu D., Chen W., Zhu N., *Advanced Control of Doubly Fed Induction Generator For Wind Power Systems*, Wiley-IEEE Press (2018), DOI: 10.1002/9781119172093.

[10] Kerrouche KDE., Mezouar A., Boumediene L., Van Den Bossche A., *Modeling and Lyapunov-designed based on adaptive gain sliding mode control for wind turbines*, Journal of Power Technologies, vol. 96, no. 2, pp. 124–136 (2016).

[11] Iov F., Hansen AD., Sørensen P., Blaabjerg F., *Wind Turbine Blockset in Matlab/Simulink*, General Overview and Description of the Models, Aalborg University and RISØ National Laboratory, Denmark (2004).

[12] Zouggar E.O., Chaouch S., Abdelhamid L., Abdeslam D.O., *Real-time implementation of the MPPT control algorithms of a wind energy conversion system by the digital simulator OPAL_RT*, European Journal of Electrical Engineering, vol. 23, no. 1, pp. 45–52 (2021), DOI: 10.18280/ejee.230106.

[13] Matthew K., Saravanakumar R., *Design of Double Integral Sliding Mode Control for Variable Speed Wind Turbine at Partial Load Region*, IEEE International Conference on Computational Intelligence and Computing Research (ICCIC), Coimbatore, India, pp. 1–5 (2017), DOI: 10.1109/ICCIC.2017.8524196.

[14] Mohamed H., Abdelmadjid B., Lotfi B., *Improvement of direct torque control performances for induction machine using a robust backstepping controller and a new stator resistance compensator*, European Journal of Electrical Engineering, vol. 22, no. 2, pp. 137–144 (2020), DOI: 10.18280/ejee.220207.

[15] Kelkoul B., Boumediene A., *Stability analysis and study between classical sliding mode control (SMC) and super twisting algorithm (STA) for doubly fed induction generator (DFIG) under wind turbine*, Energy, vol. 214, p. 118871 (2021), DOI: 10.1016/j.energy.2020.118871.

[16] Baghli L., *Contribution à La Commande de La MAS, Utilisation de La Logique Floue, Des Réseaux de Neurones et Des Algorithmes Génétiques*, PhD Thesis, Université de lorraine (1999).

[17] Mousakazemi S., Mohammad H., *Comparison of the error-integral performance indexes in a GA-tuned PID controlling system of a PWR-type nuclear reactor point-kinetics model*, Progress in Nuclear Energy, vol. 132, ISSN 0149-1970 (2021), DOI: 10.1016/j.pnucene.2020.103604.

www.czasopisma.pan.pl PAN POLSKA AKADEMIA NAUK www.journals.pan.pl

[18] Almabrok A., Psarakis M., Dounis A., *Fast Tuning of the PID Controller in An HVAC System Using the Big Bang–Big Crunch Algorithm and FPGA Technology*, Algorithms, vol. 11, no. 10, 146 (2018), DOI: 10.3390/a11100146.

[19] Zeghdi Z., Barazane L., Bekakra Y., Larabi A., *Improved Backstepping Control of a DFIG based Wind Energy Conversion System using Ant Lion Optimizer Algorithm*, Periodica Polytechnica Electrical Engineering and Computer Science, vol. 66, no. 1, pp. 43–59 (2022), DOI: 10.3311/PPee.18716.

[20] Taoussi M., Bossoufi B., Bouderbala M., Motahhir S., Alkhammash E.H., Masud M., Zinelaabidine N., Karim M., *Implementation and Validation of Hybrid Control for a DFIG Wind Turbine Using an FPGA Controller Board*, Electronics, vol. 10, no. 24 (2021), DOI: 10.3390/electronics10243154.

[21] Salhi S., Salah S., *LQR Robust Control for Active and Reactive Power Tracking of a DFIG based WECS*, International Journal of Advanced Computer Science and Applications (IJACSA), vol. 10, no. 1 (2019), DOI: 10.14569/IJACSA.2019.0100172.

[22] Nguyen A.T., Lee C., *Sensorless Control of DFIG Wind Turbine Systems Based on SOGI and Rotor Position Correction*, IEEE Transactions on Power Electronics, vol. 36, no. 5, pp. 5486–5495 (2021), DOI: 10.1109/TPEL.2020.3027888.

[23] Lazrak A., Abbou A., *Robust Power Control of DFIG Based Wind Turbine without Currents Rotor Sensor*, International Renewable and Sustainable Energy Conference (IRSEC), Tangier, Morocco (2017), DOI: 10.1109/IRSEC.2017.8477340.

[24] Mensou S., Essadki A., Nasser T., Bououlid Idrissi B., *A direct power control of a DFIG based-WECS during symmetrical voltage dips*, Protection and Control of Modern Power Systems, vol. 5, no. 1, pp. 1–12 (2020), DOI: 10.1016/j.egyr.2016.08.001.

[25] Benzouaoui A., Zoubi A.F., Khelfi M.F., *Nonlinear control scheme based on a second order sliding mode: application to DFIG supplied by five-level PWM inverter*, International Journal of Automation and Control, vol. 13, no. 4, pp. 498−516 (2019), DOI: 10.1504/IJAAC.2019.100472.

[26] Bennouk A., Nejmi A., Ramzi M., *Stability enhancement of a wind plant based on a DFIG and a PMSM: A Lyapunov approach*, Energy Reports, vol. 4, no. 2018, pp. 13–22 (2018), DOI: 10.1016/j.egyr.2017.10.001.

[27] Hao Z., Haiying D., Baoping Z., Tong W., Changwen C., *Research on beam supply control strategy based on sliding mode control*, Archives of Electrical Engineering, vol. 69, no. 2, pp. 349–364 (2020), DOI: 10.24425/aee.2020.133030.